

X Modality Assisting RGBT Object Tracking

Zhaisheng Ding

Abstract—Learning robust multi-modal feature representations is critical for boosting tracking performance. To this end, we propose a novel X Modality Assisting Network (X-Net) to shed light on the impact of the fusion paradigm by decoupling the visual object tracking into three distinct levels, facilitating subsequent processing. Firstly, to tackle the feature learning hurdles stemming from significant differences between RGB and thermal modalities, a plug-and-play pixel-level generation module (PGM) is proposed based on self-knowledge distillation learning, which effectively generates X modality to bridge the gap between the dual patterns while reducing noise interference. Subsequently, to further achieve the optimal sample feature representation and facilitate cross-modal interactions, we propose a feature-level interaction module (FIM) that incorporates a mixed feature interaction transformer and a spatial-dimensional feature translation strategy. Ultimately, aiming at random drifting due to missing instance features, we propose a flexible online optimized strategy called the decision-level refinement module (DRM), which contains optical flow and refinement mechanisms. Experiments are conducted on three benchmarks to verify that the proposed X-Net outperforms state-of-the-art trackers.

Index Terms—RGBT tracking, knowledge distillation, multi-stage fusion, refinement mechanism.

I. INTRODUCTION

VISUAL object tracking aims to accurately predict the bounding box of an object by leveraging the rich information from dual modalities. This approach capitalizes on the complementary cues provided by both RGB and thermal images, enabling it to operate seamlessly around the clock [1]. Benefiting from the leapfrog development of deep learning and thermal imaging techniques, extensive remarkable RGBT trackers have been studied and proposed, which greatly improved the precise and success rate of object tracking, while also bolstering the application of artificial intelligence (AI) in various practical domains such as autonomous driving, military reconnaissance, and intelligent security systems [2], [3].

RGB images excel at capturing informative color features and rich texture details but are easily susceptible to environmental illumination conditions. In contrast, thermal images exhibit high stability and are insensitive to variation illumination. This type of image exhibits strong anti-interference resilience to challenging environmental factors, *i.e.* haze, rain and snow, but lacks the details of the objects. The complementary feature combination of RGB and thermal images can effectively improve the classification accuracy of hard samples, thus upgrading the accuracy of tracking [4]. Therefore, how to effectively extract and utilize the complementary information emerges as a paramount considerations in RGBT tracking [5].

Early traditional-based algorithms were based on manually extracted features, which are unable to adapt to complex environments [6]. Inspired by the successful application of deep learning (DL) methods, many RGBT trackers begin to use

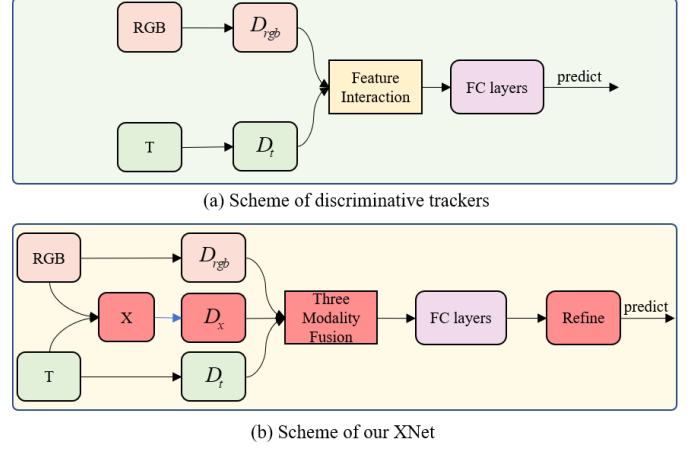


Fig. 1. Compared with existing RT-MDNet-based trackers. D_{rgb} , D_t , D_x denote the deep features of RGB, Thermal and X modality.

embedded feature fusion modules to select valid information adaptively [7], [8]. The DL-based methods, which can be broadly categorized into two branches: discriminative trackers and generative ones, usually have attribute challenge capability and are applied in a wider range of scenarios, such as drastic appearance changes, motion blur and occlusion. The Siamese network-based trackers are a common type of generative trackers. Guo et al [9] introduced a Siamese network to achieve efficient RGBT object tracking performance, which efficiently obtains the unimodal features from multimodalities by an elaborate feature fusion module. In order to fully capture cross-modal information, Zhang et al proposed a SiamCDA [10] tracker based on SiamRPN++ [11], which employs the deep network to extract the deep potential features of RGB and thermal images. Wang et al proposed a siamese-based transformer RGBT tracker to achieve feature extraction and global information interaction [12]. Hou et al proposed MTNet to explore modality-specific cues and achieve satisfactory results [13]. The Siamese network-based trackers achieve a tracking speed beyond the real-time requirement. Nevertheless, the generative trackers tend to disregard the significance of shared features across modalities, thereby posing challenges in attaining high accuracy and strong robustness.

The discrimination-based RGBT trackers have long attracted attention due to their high tracking accuracy. For instance, Li et al [14] proposed a typical kind of discriminative multi-adapter network (MANet) for RGBT tracking, which can excavate the potential value of complementary features between modalities and instance perception information through multiple convolution layers of different kernel sizes. MANet exhibits significant potential in extracting shared features. However, the repetitive utilization of large convolutional ker-

nels for feature extraction compromises network efficiency. Tu et al [15] proposed a multi-modal multi-margin metric learning (M⁵L) tracker to exploit the structural information of hard samples and achieve quality-aware fusion of complementary features. However, the performance of the M⁵L method in tracking precise and success rate is unsatisfactory, making it difficult to reach the state-of-the-art (SOTA). The mentioned methods aim to address the challenge of mining and utilizing correlation clues among different modalities, while also enhancing the anti-interference ability of the trackers. Nevertheless, there is still considerable potential for further improvement.

In summary, existing RGBT trackers still face several challenges. Firstly, there are difficulties in assessing the significance of target features present in both RGB images and infrared thermal images. Secondly, there exist challenges in efficiently exploring the correlations between different modalities of features. Lastly, existing tracking strategies lack flexibility. To handle these issues, we propose a novel X modality assisting network, termed as X-Net to reasonably adopt the interdependencies across multi-modalities. Specifically, X-Net aims to enhance tracking performance through three key improvements: pixel-level generation, feature-level interaction and decision-level refinement. As illustrated in Fig. 1, the discriminative trackers utilize a deep network to extract the deep features from both RGB and thermal images. These fused features are then fed into the classifier to predict the target’s position. The initial stage of X-Net involves generating pixel-level RGB and thermal images to obtain the X modality, which aggregates the significant complementary features of the source images. Following feature extraction and interaction, we perform prediction refinement after the classifier with the objective of enhancing tracking performance.

This paper presents the main contributions in a four-fold manner.

- 1) We propose a novel X modality assisting network (X-Net) to improve tracking performance through three key improvements: pixel-level generation, feature-level interaction and decision-level refinement.
- 2) We incorporate a lightweight pixel-level generation module (PGM) into X-Net. PGM utilizes a self-knowledge distillation to generate pixel-level feature aggregation maps. This approach effectively leverages the capabilities of a high-performance image fusion network to capture modality-shared features.
- 3) We present the feature interaction module (FIM) in conjunction with the spatial-dimensional feature translation strategy (SFTS) and the mixed feature interaction transformer (MFIT) to address variation scaling and explore cross-modal global correlations.
- 4) We design the decision-level refinement module (DRM), which combines optical flow and refinement mechanisms to optimize tracking results by the flexible tracking strategy. Comprehensive experiments verify that the proposed X-Net is superior to the state-of-the-art trackers on three RGBT benchmarks.

II. RELATED WORK

The field of RGBT tracking has witnessed significant advancements in recent years, with a key milestone being the development and release of RGBT tracking datasets. Numerous researchers have endeavored to develop deep learning-based RGBT tracking algorithms aimed at achieving high performance, which are reviewed from two perspectives as follows.

A. RGBT Tracking Methods

RGBT tracking methods can be classified into generative trackers and discriminative trackers based on their tracking mechanism. A generative RGBT tracker employs a probabilistic model to capture the correlation and joint distribution between thermal infrared and RGB pixels to implement object tracking. Siamese network-based trackers are popular in RGBT visual tracking relying on their high computing efficiency. For instance, SiamFT [16] applied the SiamFC [17] as a baseline to extract the features of multi-modalities and then fused the features by the hand-designed modality weights allocation strategy. On this basis, DSiamMFT [18] utilized the multi-level semantic features effectively and obtained a higher accuracy than SiamFT. DuSiamRT [19] adopted the channel attention module to obtain the fusion feature from the template images. SiamCDA enhanced the recognition ability of the deep features and optimized the robustness of the tracker by reducing the unimodal differences, which is based on the advanced tracker, *i.e.*, SiamRPN++. SiamCSR [20] combined the channel-spatial attention mechanism and SiamRPN++ network to implement the RGBT tracking. The Siamese network-based trackers generally have high computing efficiency and fully meet the requirements of practical applications. However, this kind of tracker is poor in processing heterogeneous RGBT data, which limits its tracking performance.

Unlike the generative RGBT tracking methods, the discriminative RGBT trackers fuse the complementary information of visible and infrared images to build a discriminant model to track the target. Generally, most of the discriminative RGBT trackers adopt the attention mechanism to strengthen the characterization of the target, which effectively classifies the target and background region. mfDiMP [21] proposed a well-designed target prediction network based on DiMP [22], and utilized the discriminant loss for end-to-end training. MANet combined attention mechanism and expanded MDNet [23] into a multi-channel network to extract the common and inherent features of multi-modalities. On this basis, MANet++ [24] enhanced the features in each modality before the fusion module to obtain better performance than MANet does. MIRNet [25] combined the self-attention and cross-attention modules to achieve a robust RGBT tracking performance. Maintaining the discrimination performance of modal features can help trackers effectively distinguish the target region from the background. Therefore, many trackers usually retain the features of RGB and TIR modes. For instance, M⁵L tracker introduced an attention-based fusion module to effectively integrate quality perception across source images, which improved the accuracy

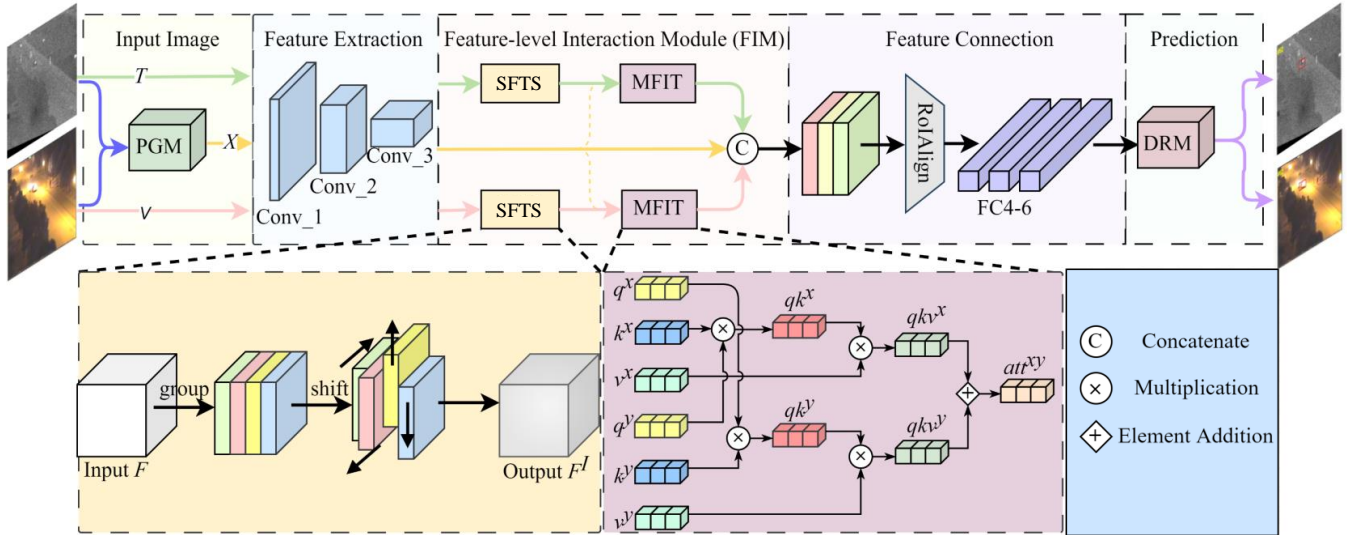


Fig. 2. Overview of the proposed X-Net framework. X-Net consists of three indivisible components, namely pixel-level generation module, feature-level interaction module and decision-level refinement module.

of object tracking. DMCNet [26] proposed a novel dual-gated mutual conditional network to take full advantage of the discriminant information of the multi-modalities while suppressing the influence of noise. ADRNet [27] and APFNet [28] focus on extracting prominent characteristics of different images and blending them to suit different attribute challenges. AGMINet [29] presented an asymmetric global and local mutual integration network to mine heterogeneous features.

B. RGBT information Fusion

Effective fusion of RGB and thermal information is a vital issue in RGBT tracking [30]. Various methods have been proposed, including element-wise summation, concatenation and content-dependency weighting-based fusion strategies. However, most existing fusion strategies overlook the feature differences between input RGB and thermal images, in fact, have distinct imaging mechanisms and exhibit significant differences in their features [31]. Directly fusing weighted unimodal RGB and thermal features leads to reduced discriminability in the fused features and decreased subsequent tracking performance. To fully leverage cross-modal features in RGB and thermal images, many RGBT information fusion methods such as Swinfusion [32], SeAFusion [33] and CMFA_Net [34] are proposed via different deep networks and obtain convincing results. All of these methods utilize the complementary characteristics of infrared images and RGB images, employing meticulously designed feature fusion modules for feature fusion.

Furthermore, it would be beneficial to explore and learn feature interaction strategies from high-performing RGBT fusion networks. Several algorithms employ knowledge distillation learning strategies, drawing inspiration from advanced feature fusion strategies of existing methods, to guide the development of their own RGBT information fusion techniques. For example, HKDnet [35] utilized a heterogeneous knowledge distillation framework to facilitate the simultaneous fusion

and super-resolution of thermal and visible images, which includes a high-resolution image fusion network referred to as the teacher network, as well as a low-resolution image fusion and super-resolution network known as the student network. The primary function of the teacher network is to perform fusion on high-resolution input images and guide the student network in acquiring the abilities of fusion and super-resolution, leading to achieving impressive visual effects while accurately preserving the natural texture details. CMD [36] tracker introduces a multi-path selection distillation module that guides a simple fusion module to learn more precise multi-modal information from a meticulously crafted fusion mechanism. The performance of an RGBT tracker can significantly deteriorate due to the attention to its feature expression capabilities.

In RGBT object tracking, discriminative trackers have longer runtimes compared to generative trackers. However, the generative trackers effectively utilize feature interactions between different modalities, resulting in more powerful and accurate characteristics. Efficient acquisition of intrinsic and shared features in multi-modal images, effectively combining and enhancing key features, as well as correct strategies for target tracking, constitute the primary tasks of discriminative trackers. These challenging tasks motivate us to propose an advanced architecture to enhance tracking performance.

III. METHODOLOGY

A. Network Architecture

The pipeline of the X-Net is illustrated in Fig. 2. Concretely, we employ the tailored lightweight VGG-M network with dilated convolution as the backbone and introduce the initial three dilated convolution layers to extract the deep features of the RGB, thermal and X modality generated by the plug-and-play pixel-level generation module (PGM). Subsequently, we propose a feature-level interaction module (FIM) combining a spatial-dimensional feature translation strategy (SFTS) and

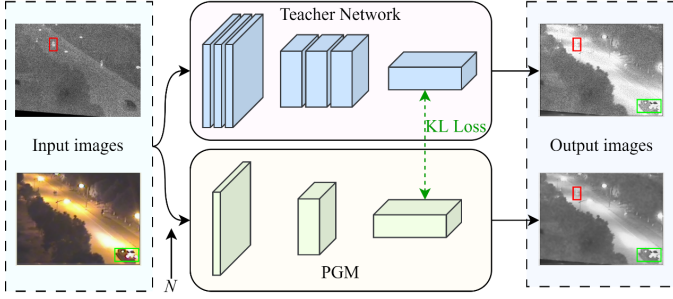


Fig. 3. The details of PGM. N denotes the noise interference.

a mixed feature interaction transformer (MFIT) to obtain an optimal feature expression. Ultimately, we proposed a decision-level refinement module (DRM) to determine the re-tracking strategy according to the confidence score and motion offset.

B. X Modality Assisting Network

Pixel-level generation module (PGM). Drawing inspiration from the strengths of infrared and visible image fusion methods, we develop a plug-and-play pixel feature representation module using self-knowledge distillation learning. The PGM integrates object cues from multi-modalities directly and reduces noise interference effectively, as shown in Fig. 3. In the process of distillation learning, the teacher network implements an advanced infrared and visible image fusion method, termed SeAFusion [37], while our PGM interacts with it as the student network for learning. The training process of PGM is shown in **Algorithm 1**. Notably, in comparison to the teacher network, the PGM has a smaller model size, fewer parameters, and lower computational costs, all while maintaining performance levels similar to that of the teacher network. The advantages of self-distillation learning empower the PGM to efficiently extract modality-shared features while simultaneously preserving rich texture details and highlighting thermal object cues.

Algorithm 1. The training process of PGM.

Input: RGB and T images
Output: fused image F

- 1: **for** $n \leq \text{max_epoch}$ **do**
- 2: **while** $k < \text{the_number_of_critic}$ **do**
- 3: Select m RGB images $\{I_{rgb}^1, \dots, I_{rgb}^m\}$;
- 4: Select m T images $\{I_t^1, \dots, I_t^m\}$;
- 5: Update output images of the teacher network $\{O_{te}^1, \dots, O_{te}^m\}$;
- 6: Select m RGB images $\{I_{rgb}^1, \dots, I_{rgb}^m\}$;
- 7: Select m T images $\{I_t^1, \dots, I_t^m\}$;
- 8: Update the PGM by Adam Optimizer;
- 9: **return** fused image X.

Feature-level interaction module (FIM). The fused image X serves as a crucial cornerstone of multi-modal representation, which synthesizes the complementary content of RGB-T images and can effectively mitigate noise interference. Subsequently, the source images RGB, T and X are fed into the feature extraction module to obtain its deep features $D_{rgb}, D_t, D_x \in \mathbb{R}^{H \times W \times C}$, where H , W and C denote the height, width and channel number of the image, respectively.

After that, we propose the FIM to strengthen the feature representation without increasing the number of learning parameters of the network. SFTS module divides the deep features D_{rgb} and D_t into four slices along the channel plane. Subsequently, these slices are shifted by a single pixel in each of the four directions of height and width, which are defined as follows:

$$\begin{cases} \overline{D_{rgb}}[:, 2 : W, 1 : C/4] \leftarrow D_{rgb}[:, 1 : W - 1, 1 : C/4] \\ \overline{D_{rgb}}[:, 1 : W - 1, C/4 + 1 : C/2] \leftarrow D_{rgb}[:, 2 : W, C/4 + 1 : C/2] \\ \overline{D_{rgb}}[2 : H, :, C/2 : 3C/4] \leftarrow D_{rgb}[1 : H - 1, :, C/2 : 3C/4] \\ \overline{D_{rgb}}[1 : H - 1, :, 3C/4 : C] \leftarrow D_{rgb}[2 : H, :, 3C/4 : C] \end{cases} \quad (1)$$

$$\begin{cases} \overline{D_t}[2 : H, :, 1 : C/4] \leftarrow D_t[1 : H - 1, :, 1 : C/4] \\ \overline{D_t}[1 : H - 1, :, C/4 + 1 : C/2] \leftarrow D_t[2 : H, :, C/4 + 1 : C/2] \\ \overline{D_t}[:, 2 : W, C/2 : 3C/4] \leftarrow D_t[:, 1 : W - 1, C/2 : 3C/4] \\ \overline{D_t}[:, 1 : W - 1, 3C/4 : C] \leftarrow D_t[:, 2 : W, 3C/4 : C] \end{cases} \quad (2)$$

The SFTS module misaligns the elements by the spatial shift to enrich the detailed textures of an object. To prevent excessive interference caused by object shifting, the SFTS module is designed to shift elements by just one pixel in space. However, in cases where two objects are in close spatial proximity, their features may intersect or overlap, leading to tracking failures. As a solution, we propose the mixed feature interaction transformer (MFIT) to fuse the features produced by the SFTS, mitigating the interference resulting from spatial displacement.

The MFIT is based on self-attention and cross-modal attention. Initially, the features $\overline{D_{rgb}}$ and $\overline{D_t}$ are reshaped to obtain their own *Query* $\{q^{rgb}, q^t \in \mathbb{R}^{HW \times C}\}$, *Key* $\{k^{rgb}, k^t \in \mathbb{R}^{HW \times C}\}$ and *Value* $\{v^{rgb}, v^t \in \mathbb{R}^{HW \times C}\}$, respectively. Subsequently, the cross-modal attention map is calculated by the following formulas:

$$D_{rgb-t} = \text{softmax} \left(\frac{q^t (k^{rgb})^T}{\sqrt{d_k}} \right) v^{rgb} \quad (3)$$

$$D_{t-rgb} = \text{softmax} \left(\frac{q^{rgb} (k^t)^T}{\sqrt{d_k}} \right) v^t \quad (4)$$

where $\{D_{rgb-t}, D_{t-rgb} \in \mathbb{R}^{H \times W \times C}\}$ stands for a pair of attention maps, and d_k denotes the scaling factor, set as 1. Ultimately, adding the attention maps and linking with the deep fusion features D_X to obtain the informative fusion maps $\overline{D_f} \in \mathbb{R}^{H \times W \times 2C}$.

$$Att^{rgbt} = D_{rgb-t} + D_{t-rgb} \quad (5)$$

$$\overline{D_f} = \text{concat}(D_x, Att^{rgbt}) \quad (6)$$

The feature visualization of the FIM is depicted in Fig. 4. It is evident that the inclusion of FIM allows the tracker to effectively attend to small objects, ensuring that it can focus on minute target regions. In contrast, the absence of FIM may lead to a failure to concentrate on these small target areas.

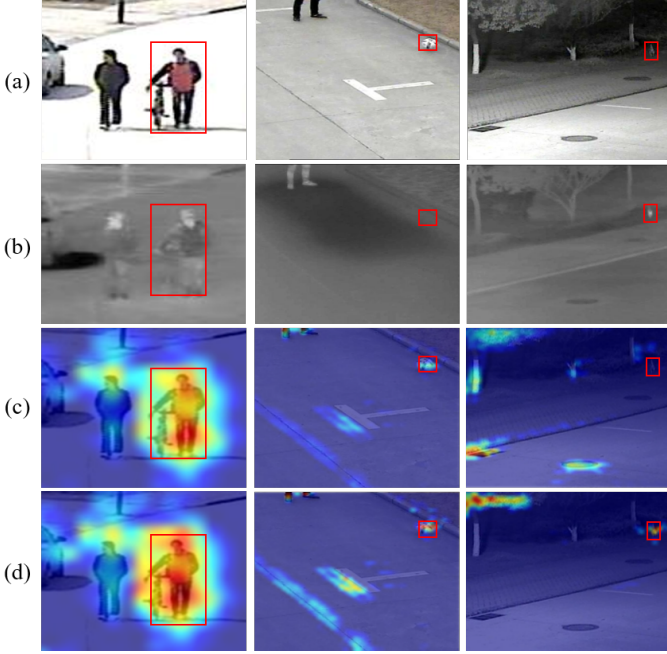


Fig. 4. Illustration of the effectiveness of feature attention in FIM. (a) RGB images, (b) Thermal images, heatmap of features (c) without FIM, (d) with FIM.

The fused feature maps are cropped by the RoIAlign and then fed into the binary classifier to obtain a coarse location. When confronted with abrupt drifts between adjacent frames, the local search strategy employed by the base tracker proves to be ineffective. Furthermore, the base tracker’s initial frame-based learning of bounding box regression is challenging to dynamically adjust the target scale in ensuing frames. Consequently, it is verified to be challenging to dynamically adjust the scale in ensuing frames.

Decision-level refinement module (DRM). To further enhance the tracking performance, we propose the DRM to optimize bounding boxes and estimate motion offsets, which implements different bounding box regression strategies based on the confidence score C_S . When $C_S < 0$, DRM applies the Lucas-Kanade optical flow [38] repositioning rule based on pyramid layering to obtain the target motion offset. The final target positioning is achieved by adding the target location obtained from the local search using Gaussian sampling to the offset in motion. If $C_S > 0$, the refinement network is initialized to consistently improve the accuracy of the predicted bounding box. In particular, we fine-tune the plug-and-play Alpha Refine [39] component on the RGBT dataset, which can refine the bounding boxes accurately with its exceptional spatial awareness capability.

C. Network Training

During the offline training phase, we utilize the VGG-M architecture as our backbone and implement a multi-domain learning strategy. Afterward, we randomly sample 8 frames and extract 32 positive samples and 96 negative samples per frame using Intersection over Union (IoU) and Gaussian distribution. These samples are employed to construct a mini-

batch. We optimize our network using the AdamW and set the learning rate for the convolution layers to $1e^{-4}$, for the fully connected layers to $1e^{-4}$, and the training epoch to 200.

D. Online Tracking

Algorithm 2. The online tracking process of X-Net.

Input: All pre-trained parameters of the backbone.

Original target position Z_1 .

Output: Predicted target position Z_t^*

1: Initialize the parameters of W_{fc6} ;

2: Train the bounding box regressor $BR(\cdot)$;

3: Generate positive and negative samples S_1^+, S_1^- ;

4: Renew $W_{fc4-fc6}$ through S_1^+, S_1^- ;

5: Generate short-term and long-term samples U_s, U_l .

6: **repeat**

7: Draw candidate samples z_t^i .

8: Calculate the optimum target state Z_t^* .

9: **if** $f^+(Z_t^*) > 0.5$ **then**

10: Generate training samples S_t^+, S_t^- ;

11: Computing $Z_t^* = BR(Z_t^*)$;

12: Update U_s, U_l .

13: **if** $f^+(Z_t^*) < 0.5$ **then**

14: Execute short-term update $W_{fc4-fc6}$ with U_s .

15: **else if** $t\%10 = 0$ **then**

16: Execute long-term update $W_{fc4-fc6}$ with U_l .

17: **if** $C_S > 0$ **then**

18: Obtain the refine target position Z_m^* .

19: **else if** $C_S < 0$ **then**

20: Calculate the average displacement vector $[x^*, y^*]$.

21: Obtain the predict target position Z_m^* .

22: Improve Z_m^* to Z_t^* .

23: **until** termination of sequence.

Algorithm 2 illustrates the complete online tracking process. Concretely, the fully connected (FC) layers in the backbone are updated while other parameters remain fixed. From the starting gate, X-Net is initialized on the first frame of the sequence with the target position. Gaussian sampling is performed around the target in the first frame to obtain 500 positive samples S_1^+ with IoU > 0.7 , and 5000 negative samples S_1^- with IoU < 0.5 w.r.t the ground truth. The FC layers undergo 50 epochs of fine-tuning based on these samples, with a learning rate of $1e^{-4}$ for FC6 and $1e^{-3}$ for the remaining layers. A total of 1000 samples are chosen for training the bounding box regressor with the objective of obtaining a precise bounding box that encompasses the target. In order to mitigate the impact of tracking inefficiency and inaccurate predictions for subsequent video frame tracking boxes, the regressor is trained only using the initial frame and the corresponding bounding box. The regression model modifies the tracking coordinates of subsequent frames to achieve more accurate tracking. Thereafter, both short- and long-term updates are conducted using a set of 50 positive samples S_t^+ and 200 negative samples S_t^- . A Gaussian sampling technique is utilized with Z_{t-1}^n as the center to generate 256 candidate regions Z_t^i for the t th frame. The trained network evaluates the positive scores $f^+(Z_t^i)$ and negative scores $f^-(Z_t^i)$ for each of these candidate samples. Subsequently, the confidence scores of the candidates are sorted and the top 5 candidates

TABLE I
COMPARISON RESULTS OF THE PROPOSED METHOD AGAINST THE STATE-OF-THE-ART TRACKERS. OVERALL PERFORMANCE IS EVALUATED BY PR/SR SCORES (%) AND IS PRODUCED ON GTOT. THE BEST RESULTS ARE MARKED IN RED.

Trackers	MIRNet	APFNet	AGMINet	MFGNet	SiamCDA	HDINet	MSIFNet	RPCF	M2GCI	EDFNet	DMSTM	X-Net
ALL	90.9/74.4	90.4/73.5	91.7/73.4	80.3/65.3	87.7/73.2	88.8/71.8	90.4/74.1	92.7/64.6	90.9/73.7	91.2/74.6	92.9/75.9	93.1/76.7

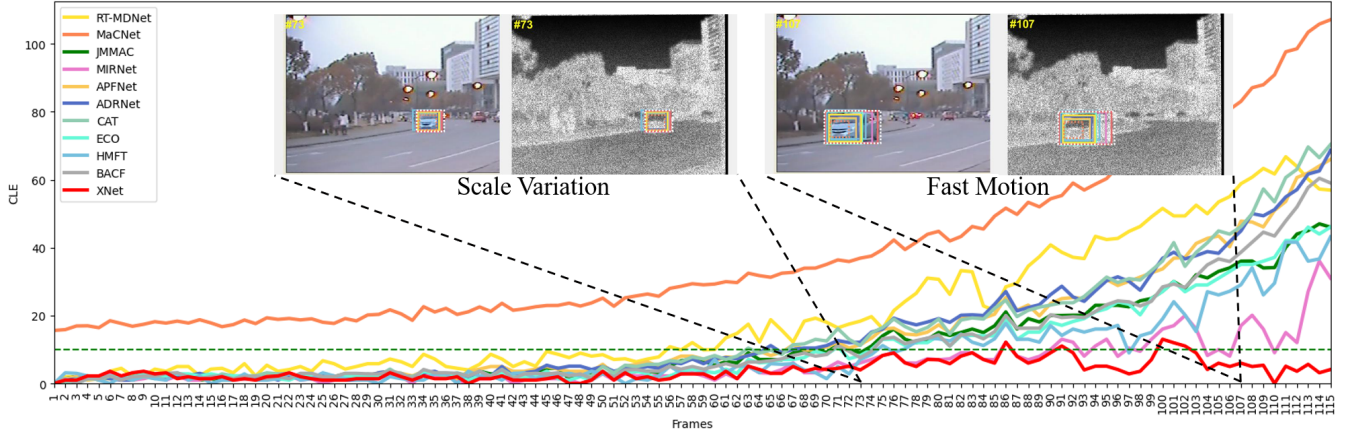


Fig. 5. Comparison results of X-Net against the state-of-the-art trackers. Challenge-based performance is evaluated by PR/SR scores (%) and produced on GTOT.

with the highest scores are selected and averaged as the set Z_m^* . Ultimately, the DRM is employed as the optimization metric for refining the bounding box.

IV. EXPERIMENTAL RESULTS

The X-Net is implemented on the PyTorch 1.10 platform with one NVIDIA RTX3090 GPU with 24GB memory.

A. Datasets and Metrics

In this paper, we conduct comparative experiments with high-performance competitors on three RGBT benchmarks, namely GTOT [40], RGBT234 [41], and LasHeR [42]. Following established practices in the field, we employed two standard metrics, namely Precision Rate (PR) and Success Rate (SR), to demonstrate the superiority of the proposed method. We set the threshold to 5 pixels for GTOT and 20 pixels for RGBT234/LasHeR, considering the diverse image resolutions present in different datasets.

B. Evaluation on GTOT Dataset

1) **Overall performance.** The proposed tracker is compared with 11 state-of-the-art RGBT methods, i.e., MIRNet, APFNet, AGMINet, MFGNet [43], SiamCDA, HDINet [44], MSIFNet [45], RPCF [46], M2GCI [47], EDFNet [48] and DMSTM [49]. As reported in Table I, X-Net exhibits superior tracking capability compared to the state-of-the-art trackers, with PR of 93.1%, surpassing the compared trackers by approximately 0.4%-12.8%. Moreover, with regards to the SR, X-Net outperforms compared trackers, obtaining an impressive SR of 76.7%. The results demonstrate that X-Net is capable of attaining exceptional performance.

2) **Challenge-based performance.** To evaluate the superiority and robustness of the designed methodology, we conduct

challenge-based performance tested on the GTOT dataset and compared with 11 excellent RGBT trackers, including CAT [50], APFNet, ADRNet, HMFT [51], JMMAC [52], MaCNet, MIRNet, BACF [53], ECO [54], RT-MDNet [55] and SiamDW [56]. The visualization of the results of the attribute challenge is shown in Fig. 5, and the lines represent the Euclidean distance between the predicted centroid point of the compared methods and the ground truth. It can be observed that the prediction of X-Net is always closer to the ground truth bounding box than the comparisons, regardless of whether facing scale variation (SV) and fast motion (FM) challenges. The tracking performance of 7 challenges of deformation (DEF), large scale variation (LSV), occlusion (OCC), fast motion, low illumination (LI), thermal crossover (TC) and small object (SO) is shown in Fig. 6. Clearly, the proposed method excels in the challenges of OCC, LSV, LI, TC and SO both in PR and SR, which indicates X-Net is exceptional resistance to interference and versatility across diverse scenarios. Besides, X-Net demonstrates optimal or near-optimal performance in addressing the DEF and FM challenges, showcasing accurate target tracking capabilities despite the target undergoing various transformations. In conclusion, the proposed tracker X-Net exhibits a distinct octagonal shape in the radar chart visualization of the GTOT dataset, providing a more comprehensive representation in comparison to the other methods. The results demonstrate the capability of X-Net to effectively address multiple challenges and achieve outstanding performance, highlighted by its remarkable robustness.

3) **Qualitative comparison.** In order to comprehensively showcase the benefits of X-Net, a qualitative comparison of the tracking results on *GarageHover*, *BlackSwan1* and *Fast-motorNig* sequences is conducted with 10 exemplary trackers, as shown in Fig. 7. Specifically, the *GarageHover* sequence reveals the inability of the ECO and BACF methods to track

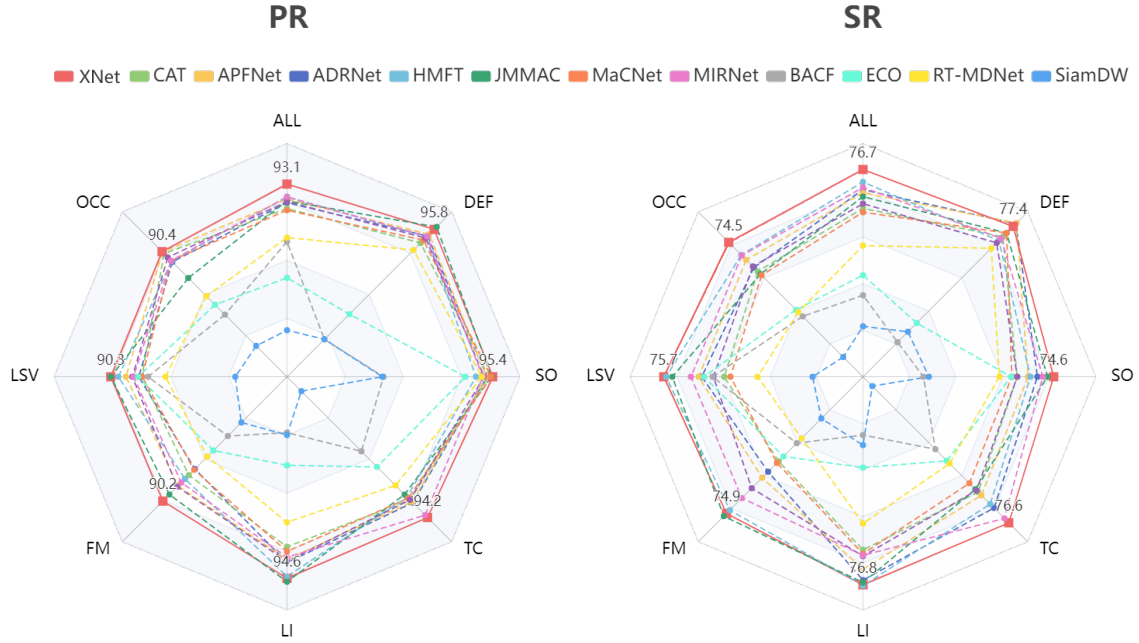


Fig. 6. Visualization of the results of attribute challenge.

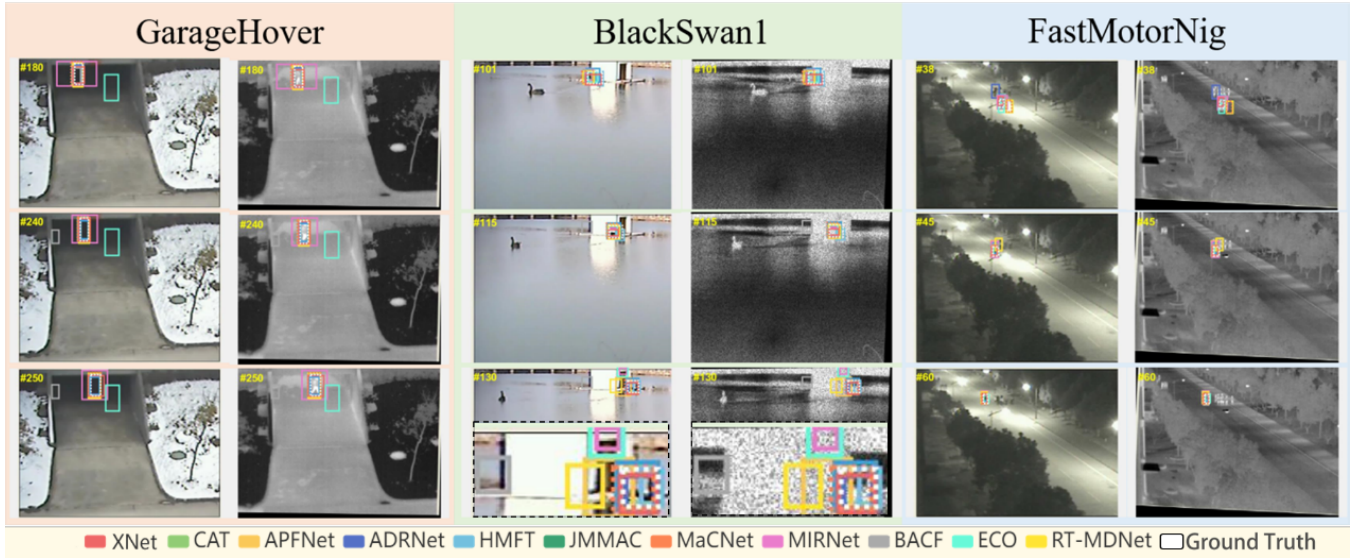


Fig. 7. Qualitative comparison results of different trackers on the GTOT dataset.

the object in low illumination conditions. The tracking boxes of MIRNet are noticeably inaccurate. In the case of the *BlackSwan1* sequence, the zoomed-in section of the tracking results for the 130th frame is presented in the bottom black box of the third row in the image, which illustrates the BACF, ECO, RT-MDNet, APFNet and MIRNet methods struggle to track the object when faced with background interference. In scenarios where tracking occurs during nighttime with rapid target movement (*FastMotorNig*), conventional methods commonly encounter challenges, such as imprecise tracking or even misidentifying targets. In contrast, the proposed RGBT tracker consistently achieves stable and accurate tracking performance.

C. Evaluation on RGBT234 Dataset

1) **Overall performance.** The RGBT234 dataset is applied to evaluate the performance comprehensively, as reported in Table II and Table III. It is evident that the X-Net outperforms the comparisons both in the PR and SR metrics. The proposed method surpasses the EDFNet method by 2.5% and 4.2% in terms of PR and SR, respectively. Significantly, X-Net demonstrates an improvement of approximately 17.1%/14% in PR/SR, compared to RPCF.

2) **Attribute-based performance.** The challenging attributes of the RGBT234 dataset can be categorized into 12 types, i.e., no occlusion (NO), partial occlusion (PO), heavy occlusion (HO), low illumination (LI), low resolution (LR),

TABLE II

COMPARISON RESULTS OF THE PROPOSED METHOD AGAINST THE STATE-OF-THE-ART TRACKERS. ATTRIBUTE-BASED AND OVERALL PERFORMANCE ARE EVALUATED BY PR SCORES (%) AND ARE PRODUCED ON RGBT234. THE BEST RESULTS ARE MARKED IN RED.

Trackers	NO	PO	HO	LI	LR	TC	DEF	FM	SV	MB	CM	BC	ALL
MIRNet	95.4	86.1	71.0	83.4	83.9	81.1	77.8	68.3	82.7	74.6	76.4	78.9	81.6
APFNet	94.8	86.3	73.8	84.3	84.4	82.2	78.5	79.1	83.1	74.5	77.9	81.3	82.7
AGMINet	94.9	90.2	72.9	87.0	86.7	80.6	79.5	79.4	83.2	78.2	79.0	83.3	84.0
MFGNet	92.0	84.3	66.2	79.1	79.3	81.8	72.1	72.5	76.1	73.7	73.2	74.3	78.3
SiamCDA	88.4	84.2	66.2	81.8	70.9	67.4	77.9	61.4	77.7	63.6	73.3	74.0	76.0
HDINet	88.4	84.9	67.1	77.7	80.1	77.2	76.2	71.7	77.5	70.8	69.7	71.1	78.3
MSIFNet	92.6	84.7	73.8	83.2	85.1	84.4	74.7	74.7	82.0	75.8	77.3	80.5	81.7
RPCF	81.5	71.8	58.3	64.4	62.5	64.8	65.5	55.2	70.6	58.0	61.1	56.6	68.1
HATFNet	92.1	86.0	70.3	78.4	79.6	75.5	77.4	74.0	80.9	71.1	76.7	77.9	80.7
M2GCI	88.0	82.8	71.9	75.2	78.3	74.0	75.1	69.1	80.2	70.0	69.0	77.1	79.3
EDFNet	91.5	85.3	76.2	78.4	80.4	75.2	79.9	72.1	83.8	73.6	73.6	80.3	82.7
DMSTM	90.5	79.0	72.9	78.8	75.2	72.2	80.0	76.0	54.0	72.9	76.5	72.4	78.6
X-Net	94.9	90.5	75.7	83.2	84.8	86.9	82.4	76.3	87.6	80.6	81.7	78.3	85.2

TABLE III

COMPARISON RESULTS OF THE PROPOSED METHOD AGAINST THE STATE-OF-THE-ART TRACKERS. ATTRIBUTE-BASED AND OVERALL PERFORMANCE ARE EVALUATED BY PR SCORES (%) AND ARE PRODUCED ON RGBT234. THE BEST RESULTS ARE MARKED IN RED.

Trackers	NO	PO	HO	LI	LR	TC	DEF	FM	SV	MB	CM	BC	ALL
MIRNet	72.4	62.7	49.0	57.5	56.3	59.1	58.1	47.1	61.9	54.6	55.4	51.7	58.9
APFNet	68.0	60.6	50.7	56.9	56.5	58.1	56.4	51.1	57.9	54.5	56.3	54.5	57.9
AGMINet	69.1	63.9	50.3	59.8	57.2	59.2	56.8	51.2	59.3	57.5	57.5	55.3	59.2
MFGNet	64.0	58.0	44.3	54.2	49.5	55.8	50.8	44.6	52.8	51.0	50.4	45.9	53.5
SiamCDA	66.4	63.9	48.7	61.2	49.9	47.7	59.2	45.3	59.3	47.9	54.7	52.9	56.9
HDINet	65.1	60.4	47.3	53.2	54.5	57.5	56.5	47.5	55.8	52.6	51.4	47.8	55.9
MSIFNet	66.0	59.5	50.5	55.7	56.5	59.0	53.5	47.5	57.6	54.4	54.9	52.3	57.0
RPCF	59.7	51.0	40.4	45.2	41.3	47.1	46.5	37.7	51.2	41.7	44.0	36.9	48.2
HATFNet	70.3	64.2	50.0	55.2	55.1	56.2	58.4	51.4	61.2	53.9	56.9	52.4	59.5
M2GCI	64.9	59.8	50.4	51.7	53.8	55.3	54.8	44.8	58.4	51.8	50.9	51.5	56.9
EDFNet	66.1	60.9	51.4	52.8	54.9	56.3	55.9	45.7	59.6	52.8	51.9	52.6	58.0
DMSTM	66.5	57.2	50.4	55.7	51.0	50.7	58.9	51.6	61.1	52.7	54.8	47.9	56.2
X-Net	72.7	66.7	53.1	57.2	59.3	64.4	60.9	53.1	65.6	60.2	59.8	52.7	62.2

thermal crossover (TC), DEF, fast motion (FM), scale variation (SV), motion blur (MB), camera movement (CM) and background clutter (BC). Based on the metric values presented in Table II and Table III, X-Net achieves the highest levels of accuracy and success in the challenging attributes such as NO, PO, TC, DEF, SV, MB, CM and BC. X-Net surpasses the RT-MDNet-based method AGMINet and attains PR/SR gains of 0.3%/2.8, 2.8%/2.8%, 6.3%/5.2%, 2.9%/4.1%, 4.4%/6.3%, 2.4%/2.7%, and 2.7%/2.3% for the HO, TC, DEF, SV, MB, and CM challenges, respectively. Besides, X-Net exhibits outstanding performance, with impressive PR/SR scores of 90.5%/66.7%, 86.9%/64.4%, 80.6%/60.2%, and 81.7%/59.8% when confronted with common attribute challenges including HO, TC, MB and CM, respectively. In the absence of no occlusions, the proposed tracker secures an elevated accuracy and success rate of 94.9%/72.7%. However, in the LI and BC challenges, X-Net exhibits inferior performance compared to AGMINet. This can be attributed to the ability of AGMINet to extract multi-scale information at each layer of features, allowing robust target localization even in the presence of low illumination and background clutter scenarios. The process of extracting features at each layer leads to an increase in computation complexity. X-Net exhibits exceptional competence in addressing attribute challenges, facilitating effective object tracking in diverse scenarios.

3) Qualitative comparison. Qualitative comparison experi-

ments are conducted on 9 video sequences, including *aftertree*, *baby*, *carafertree*, *dog1*, *manypeople*, *nighththreepeople*, *people1*, *soccer2* and *threeman2*, by comparing with 9 state-of-the-art trackers, as illustrated in Fig. 8. To facilitate the demonstration, we present the results using local magnification. Explicitly, in the *aftertree* sequence, the target person is effectively tracked in all comparisons for the first 140 frames. However, at 312th frame, when occluded by trees, the majority of trackers, specifically the ECO and HMFT methods, display tracking errors or inaccuracies. In the *baby* sequence, the tracked target encounters attributes such as scale variation, occlusion, and thermal overlap as it approaches. The effects of tracking by different trackers are particularly notable. For example, most of the trackers have already encountered issues of tracking the wrong target at 290th frame, and only MIRNet, ADRNet and X-Net are able to track the target at 537th frame. The target areas tracked by the MIRNet and ADRNet methods are significantly larger than the intended tracking area, while X-Net achieves the highest accuracy. Both camera movement and scale variation attributes are present in the sequences featuring *carafertree* and *dog1*, leading to the difficulty of correctly tracking the target. The proposed method demonstrates accurate tracking of a car or dog, even during motion and partial occlusion. In the *manypeople*, *people1* and *threeman2* sequences, the target faces challenges associated with occlusion and thermal overlap during the tracking pro-

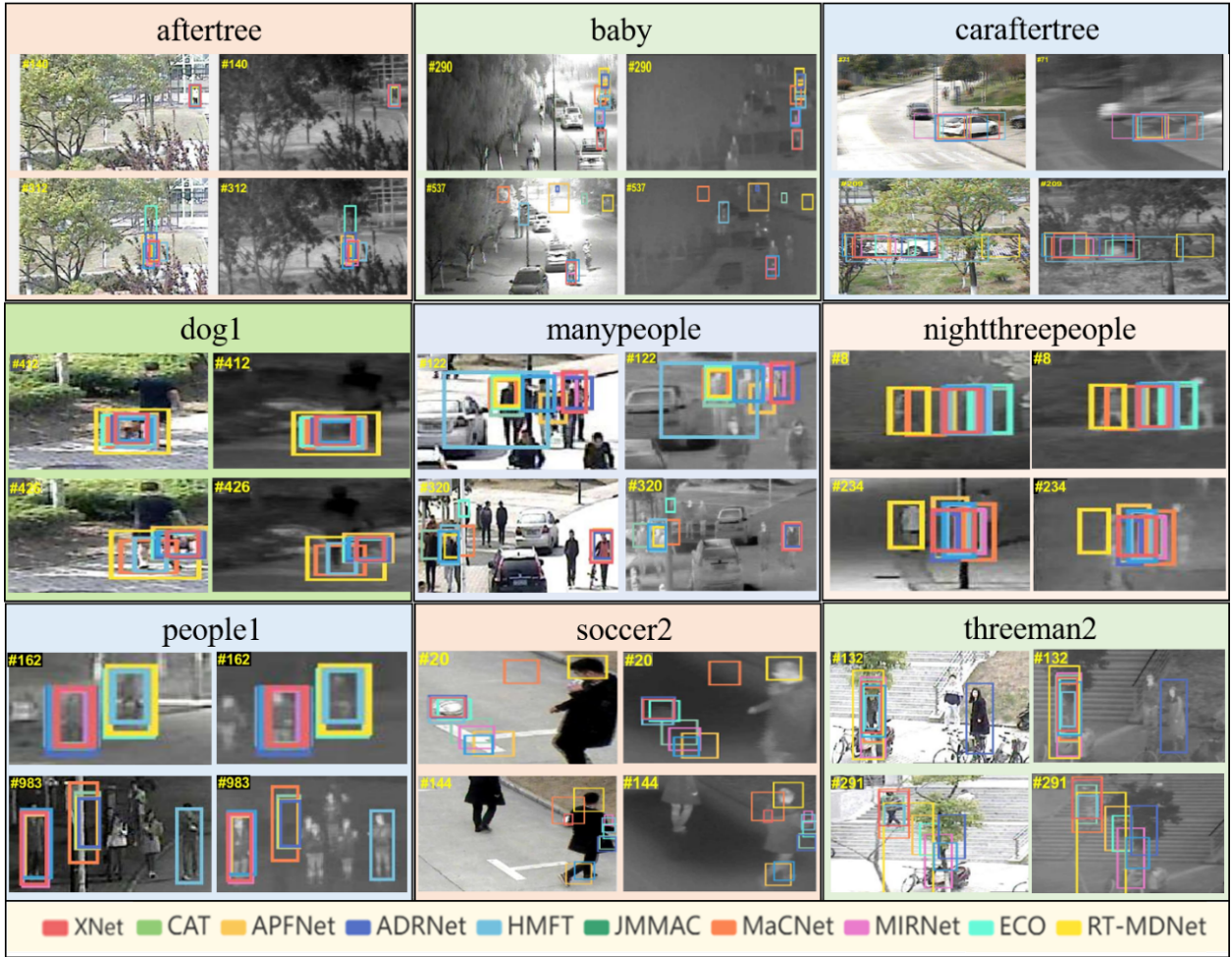


Fig. 8. Qualitative comparison results of different trackers on the RGBT234 dataset.

cess. Additionally, significant interference from surrounding persons adversely affects the performance of the trackers. The results from the two sequences demonstrate that X-Net consistently and accurately tracks the target without being affected by interference. When dealing with a rapidly moving soccer target, it becomes evident that most trackers struggle to accurately track the soccer within the first 20 frames. However, the proposed X-Net method proves to be the exception, successfully and precisely tracking the soccer by the 144th frame. While the other tracking methods being compared produce inaccurate results, X-Net consistently delivers precise and reliable tracking results.

In summary, the proposed method has consistently achieved exceptional tracking results on the challenging RGBT234 dataset, further confirming its superior tracking performance and robustness in various challenging scenarios. In medium-to-long video sequence tracking, X-Net surpasses the comparison methods, showcasing exceptional stability.

D. Evaluation on LasHeR Dataset

To further validate the robustness of X-Net, the model is trained on the RGBT234 dataset and evaluated on the testing subset of LasHeR. The comparison results of X-Net against 13

existing trackers, *i.e.*, APFNet, DMCNet, MaCNet, mfDiMP, MANet, CAT, DAPNet [57], MANet++, DAFNet [58], FANet [59], CMR [60], SGT++ and SGT [61], is shown in Fig. 9, which demonstrates the proposed method performs optimal in terms of PR and SR. Specifically, X-Net demonstrates superior performance over the SGT method with improvements of 18.1% and 20.4% in PR and SR metrics, respectively. Additionally, it achieves 4.1% and 10.2% higher PR and SR metrics compared to the MANet++ algorithm. In conclusion, the proposed X-Net demonstrates competitive tracking performance on LasHeR datasets, confirming its effectiveness, robustness and ability to handle attribute challenges across diverse datasets.

E. Efficiency Analysis

Tracking efficiency is critical for trackers and serves as a fundamental metric for their evaluation. In order to conduct a comprehensive evaluation of X-Net, we benchmark its speed against six trackers on the GTOT dataset, as displayed in Fig. 10. It can be observed that X-Net demonstrates strong competitiveness in terms of performance and speed. Specifically, X-Net achieves a tracking speed of 21 ± 3 fps, which are 7 and 9.5 times faster than those of the MANet and DMCNet,

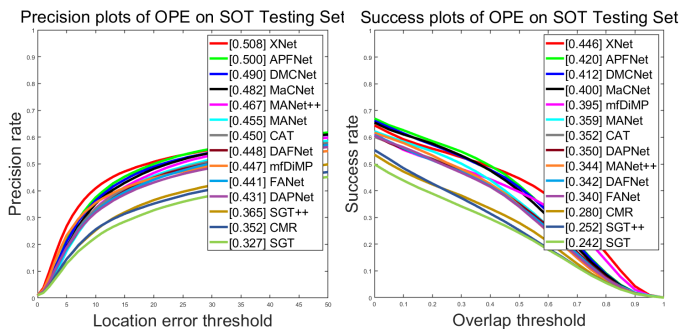


Fig. 9. Comparison results of X-Net against the state-of-the-art trackers. Overall performance is evaluated by PR/SR scores (%) and is produced on LasHeR.

respectively. Notably, X-Net outperforms both DAFNet and MIRNet in terms of PR/SR metrics, even though it shows marginally slower execution speed.

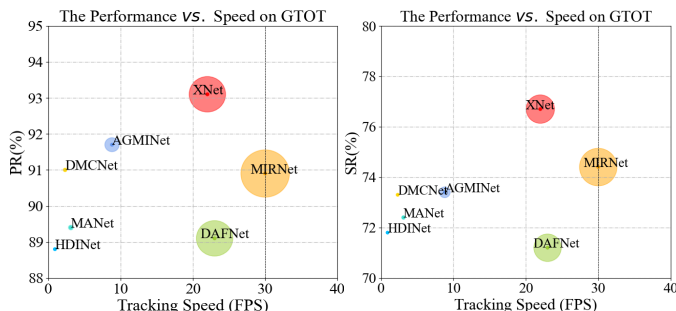


Fig. 10. Illustration of the efficiency of X-Net against six trackers.

TABLE IV

COMPARISON RESULTS OF THE PROPOSED METHOD AGAINST THE STATE-OF-THE-ART TRACKERS. ATTRIBUTE-BASED AND OVERALL PERFORMANCE ARE EVALUATED BY PR SCORES (%) AND ARE PRODUCED ON GTOT AND RGBT234. THE BEST RESULTS ARE MARKED IN RED.

	MANet	HDINet	DMCNet	AGMNet	X-Net
Flops (GB)	0.28	0.27	0.94	0.35	0.68
Params (MB)	7.11	9.40	11.45	10.76	6.93

Moreover, we compare two crucial network metrics, namely Flops and Params, to measure the complexity of the proposed model. Table IV displays that the proposed method has lower parameters compared with the comparison methods, indicating the minimal space complexity of X-Net. It can be concluded that the X-Net model proposed in this study demonstrates lower Flops compared to DMCNet, showcasing its competitive advantage.

F. Ablation Study

To validate the feasibility of each contribution, we implement four variants and test them on the GTOT and RGBT234 dataset, *i.e.*, X-Net-v1 is a base model, which fuses RGB and thermal features via simple element addition. X-Net-v2 incorporates the PGM into the baseline network. X-Net-v3 combines the PGM and FIM into the baseline tracker. X-Net is the final version equipped with all of the contributions.

The ablation results of different variants are reported in Table V, and we can draw the following conclusions: 1) Each proposed improvement significantly enhances the performance of the tracker. 2) By effectively leveraging the fused features from dual modalities, the PGM greatly improves the tracking precision and success rate of the baseline network. 3) The FIM effectively utilizes cues between modality space features to enhance the perception of modality, thereby improving the accuracy of localization. 4) The proposed DRM not only prevents misalignment but also contributes to achieving optimal tracking results.

TABLE V

COMPARISON RESULTS OF THE PROPOSED METHOD AGAINST THE STATE-OF-THE-ART TRACKERS. ATTRIBUTE-BASED AND OVERALL PERFORMANCE ARE EVALUATED BY PR SCORES (%) AND ARE PRODUCED ON GTOT AND RGBT234. THE BEST RESULTS ARE MARKED IN RED.

Variants	PGM	FIM	DRM	GTOT	RGBT234
X-Net-v1				74.5/63.1	71.4/50.0
X-Net-v2	✓			83.6/68.7	74.5/54.7
X-Net-v3	✓	✓		90.4/74.5	78.8/57.6
X-Net	✓	✓	✓	93.1/76.7	85.2/62.2

V. CONCLUSION

A high-performance X-Net is proposed to effectively address the RGBT tracking task. By integrating three meticulously crafted and impactful design modules, including PGM, FIM and DRM, X-Net demonstrates a significant enhancement in tracking performance. Firstly, the PGM is proposed to integrate object cues from multi-modalities directly and reduce noise interference effectively, which is a plug-and-play pixel feature representation module via self-knowledge distillation learning. Secondly, to effectively address the scale changes and construct the cross-modal communication relationship of multi-modal deep features, we propose the FIM combining a spatial-dimensional shift strategy and a mixed feature interaction transformer. Finally, the DRM is proposed to determine the re-tracking strategy by adopting a refinement strategy and optical flow algorithm. Experimental results on three benchmark datasets demonstrate that the proposed X-Net outperforms the state-of-the-art trackers. In further work, our study aims to investigate the crucial cues provided by multi-modal features that impact tracking performance, and develop the knowledge distillation-based theoretical framework in the field of RGBT tracking.

ACKNOWLEDGMENTS

This work is supported by the National Natural Science Foundation of China (Nos. 62266049). "Famous teacher of teaching" of Yunnan 10000 Talents Program. Key project of Basic Research Program of Yunnan Province (No. 202101AS070031). General project of National Natural Science Foundation of China (No. 81771928).

REFERENCES

- [1] Q. Xu, Y. Mei, J. Liu and C. Li, "Multimodal Cross-Layer Bilinear Pooling for RGBT Tracking," IEEE Transactions on Multimedia, vol. 24, pp. 567-580, 2022.

- [2] J. Peng, H. Zhao, and Z. Hu, "Dynamic fusion network for RGBT tracking," *IEEE Transactions on Intelligent Transportation Systems*, vol. 24, no. 4, pp. 3822-3832, 2022.
- [3] A. Lu, C. Qian, C. Li, J. Tang, and L. Wang, "Duality-gated mutual condition network for RGBT tracking," *IEEE Transactions on Neural Networks Learning Systems*, pp. 1-14, 2022.
- [4] J. Qiu, R. Yao, Y. Zhou, P. Wang, Y. Zhang, and H. Zhu, "Visible and Infrared Object Tracking via Convolution-Transformer Network With Joint Multimodal Feature Learning," *IEEE Geoscience Remote Sensing Letters*, vol. 20, pp. 1-5, 2023.
- [5] Z. Cheng, A. Lu, Z. Zhang, C. Li, and L. Wang, "Fusion Tree Network for RGBT Tracking," in *2022 18th IEEE International Conference on Advanced Video and Signal Based Surveillance (AVSS)*, Madrid, Spain, 2022, pp. 1-8.
- [6] M. Feng and J. Su, "Learning Multi-Layer Attention Aggregation Siamese Network for Robust RGBT Tracking," in *IEEE Transactions on Multimedia*, pp. 1-15, 2023.
- [7] C. Li, C. Zhu, J. Zhang, B. Luo, X. Wu, and J. Tang, "Learning Local-Global Multi-Graph Descriptors for RGB-T Object Tracking," *IEEE Transactions on Circuits and Systems for Video Technology*, vol. 29, no. 10, pp. 2913-2926, 2019.
- [8] K. Song, W. Zhang, W. Lu, Z. J. Zha, X. Ji, and Y. Li, "Visual Object Tracking via Guessing and Matching," *IEEE Transactions on Circuits and Systems for Video Technology*, vol. 30, no. 11, pp. 4182-4191, 2020.
- [9] D. Guo, J. Wang, Y. Cui, Z. Wang, and S. Chen, "SiamCAR: Siamese Fully Convolutional Classification and Regression for Visual Tracking," in *2020 IEEE/CVF Conference on Computer Vision and Pattern Recognition (CVPR)*, 2020, pp. 6268-6276.
- [10] T. Zhang, X. Liu, Q. Zhang, and J. Han, "SiamCDA: Complementarity- and Distractor-Aware RGB-T Tracking Based on Siamese Network," *IEEE Transactions on Circuits and Systems for Video Technology*, vol. 32, no. 3, pp. 1403-1417, 2022.
- [11] B. Li, W. Wu, Q. Wang, F. Zhang, J. Xing, and J. Yan, "Siamrpn++: Evolution of siamese visual tracking with very deep networks," in *Proceedings of the IEEE/CVF conference on computer vision and pattern recognition*, 2019, pp. 4282-4291.
- [12] F. Wang, W. Wang, L. Liu, et al. "Siamese transformer RGBT tracking," *Appl Intell*, vol. 53, pp. 24709-24723, 2023.
- [13] R. Hou, B. Xu, T. Ren and G. Wu, "MTNet: Learning Modality-aware Representation with Transformer for RGBT Tracking," *2023 IEEE International Conference on Multimedia and Expo (ICME)*, Brisbane, Australia, 2023, pp. 1163-1168.
- [14] C. L. Li, A. Lu, A. H. Zheng, Z. Tu, and J. Tang, "Multi-Adapter RGBT Tracking," in *2019 IEEE/CVF International Conference on Computer Vision Workshop (ICCVW)*, 2019, pp. 2262-2270.
- [15] Z. Tu, C. Lin, W. Zhao, C. Li, and J. Tang, "M 5 l: multi-modal multi-margin metric learning for RGBT tracking," *IEEE Transactions on Image Processing*, vol. 31, pp. 85-98, 2021.
- [16] X. Zhang, P. Ye, S. Peng, J. Liu, K. Gong, and G. Xiao, "SiamFT: An RGB-Infrared Fusion Tracking Method via Fully Convolutional Siamese Networks," *IEEE Access*, vol. 7, pp. 122122-122133, 2019.
- [17] L. Bertinetto, J. Valmadre, J. F. Henriques, A. Vedaldi, and P. H. S. Torr, "Fully-Convolutional Siamese Networks for Object Tracking," *Cham*, 2016, pp. 850-865: Springer International Publishing.
- [18] X. Zhang, P. Ye, S. Peng, J. Liu, and G. Xiao, "DSiamMFT: An RGB-T fusion tracking method via dynamic Siamese networks using multi-layer feature fusion," *Signal Processing: Image Communication*, vol. 84, p. 115756, 2020.
- [19] C. Guo, D. Yang, C. Li, and P. Song, "Dual Siamese network for RGBT tracking via fusing predicted position maps," *The Visual Computer*, vol. 38, no. 7, pp. 2555-2567, 2022.
- [20] C. Guo and L. Xiao, "High Speed and Robust RGB-Thermal Tracking via Dual Attentive Stream Siamese Network," in *IGARSS 2022 - 2022 IEEE International Geoscience and Remote Sensing Symposium*, 2022, pp. 803-806.
- [21] L. Zhang, M. Danelljan, A. Gonzalez-Garcia, J. v. d. Weijer, and F. S. Khan, "Multi-Modal Fusion for End-to-End RGB-T Tracking," in *2019 IEEE/CVF International Conference on Computer Vision Workshop (ICCVW)*, 2019, pp. 2252-2261.
- [22] G. Bhat, M. Danelljan, L. V. Gool, and R. Timofte, "Learning Discriminative Model Prediction for Tracking," in *2019 IEEE/CVF International Conference on Computer Vision (ICCV)*, 2019, pp. 6181-6190.
- [23] H. Nam, and B. Han, "Learning Multi-domain Convolutional Neural Networks for Visual Tracking," in *2016 IEEE Conference on Computer Vision and Pattern Recognition (CVPR)*, 2016, pp. 4293-4302.
- [24] H. Zhang, L. Zhang, L. Zhuo, and J. Zhang, "Object tracking in RGB-T videos using modal-aware attention network and competitive learning," *Sensors*, vol. 20, no. 2, p. 393, 2020.
- [25] R. Hou, T. Ren, and G. Wu, "MIRNet: A Robust RGBT Tracking Jointly with Multi-Modal Interaction and Refinement," in *2022 IEEE International Conference on Multimedia and Expo (ICME)*, 2022, pp. 1-6.
- [26] M. Wang, H. Cai, Y. Dai, and M. Gong, "Dynamic Mixture of Counter Network for Location-Agnostic Crowd Counting," in *2023 IEEE/CVF Winter Conference on Applications of Computer Vision (WACV)*, 2023, pp. 167-177.
- [27] P. Zhang, D. Wang, H. Lu, and X. Yang, "Learning Adaptive Attribute-Driven Representation for Real-Time RGB-T Tracking," *International Journal of Computer Vision*, vol. 129, no. 9, pp. 2714-2729, 2021.
- [28] Y. Xiao, M. Yang, C. Li, L. Liu, and J. Tang, "Attribute-Based Progressive Fusion Network for RGBT Tracking," *Proceedings of the AAAI Conference on Artificial Intelligence*, vol. 36, no. 3, pp. 2831-2838, 2022.
- [29] J. Mei, Y. Liu, C. Wang, D. Zhou, R. Nie, and J. Cao, "Asymmetric Global-Local Mutual Integration Network for RGBT Tracking," *IEEE Transactions on Instrumentation and Measurement*, vol. 71, pp. 1-17, 2022.
- [30] W. Xia and D. Zhou and J. Cao and Y. Liu and R. Hou, "CIRNet: An improved RGBT tracking via cross-modality interaction and re-identification," *Neurocomputing*, vol. 439, pp. 327-339, 2022.
- [31] R. Hou, D. Zhou, R. Nie, D. Liu, L. Guo and C. Yu, "VIF-Net: An Unsupervised Framework for Infrared and Visible Image Fusion," in *IEEE Transactions on Computational Imaging*, vol. 6, pp. 640-651, 2020.
- [32] J. Ma, L. Tang, F. Fan, J. Huang, X. Mei and Y. Ma, "SwinFusion: cross-domain long-range learning for general image fusion via swin transformer," *IEEE/CAA Journal of Automatica Sinica*, vol. 9, pp. 1200-1217, 2022.
- [33] L. Tang, J. Yuan and J. Ma, "Image fusion in the loop of high-level vision tasks: A semantic-aware real-time infrared and visible image fusion network," *Information fusion*, vol. 82, pp. 28-42, 2022.
- [34] Z. Ding, H. Li, D. Zhou, H. Li, Y. Liu and R. Hou, "CMFA_Net: A cross-modal feature aggregation network for infrared-visible image fusion," *infrared physics and technology*, vol. 118, pp. 103905-, 2021.
- [35] W. Xiao, Y. Zhang, H. Wang, F. Li and H. Jin, "Heterogeneous knowledge distillation for simultaneous infrared-visible image fusion and super-resolution," in *IEEE Transactions on Instrumentation and Measurement*, vol. 71, pp. 1-15, 2022.
- [36] T. Zhang, H. Guo, Q. Jiao, Q. Zhang and J. Han, "Efficient RGB-T tracking via cross-modality distillation," in *Proceedings of the IEEE/CVF Conference on Computer Vision and Pattern Recognition (CVPR2023)*, 2023, pp. 5404-5413.
- [37] L. Tang, J. Yuan, and J. Ma, "Image fusion in the loop of high-level vision tasks: A semantic-aware real-time infrared and visible image fusion network," *Information Fusion*, vol. 82, pp. 28-42, 2022.
- [38] N. Sharmin and R. Brad, "Optimal Filter Estimation for Lucas-Kanade Optical Flow," vol. 12, no. 9, pp. 12694-12709, 2012.
- [39] B. Yan, X. Zhang, D. Wang, H. Lu, and X. Yang, "Alpha-Refine: Boosting Tracking Performance by Precise Bounding Box Estimation," in *2021 IEEE/CVF Conference on Computer Vision and Pattern Recognition (CVPR)*, 2021, pp. 5285-5294.
- [40] C. Li, H. Cheng, S. Hu, X. Liu, J. Tang, and L. Lin, "Learning Collaborative Sparse Representation for Grayscale-Thermal Tracking," *IEEE Transactions on Image Processing*, vol. 25, no. 12, pp. 5743-5756, 2016.
- [41] C. Li, X. Liang, Y. Lu, N. Zhao, and J. Tang, "RGB-T object tracking: Benchmark and baseline," *Pattern Recognition*, vol. 96, p. 106977, 2019.
- [42] C. Li et al., "LasHeR: A large-scale high-diversity benchmark for RGBT tracking," *IEEE Transactions on Image Processing*, vol. 31, pp. 392-404, 2021.
- [43] X. Wang, X. Shu, S. Zhang, B. Jiang, Y. Wang, Y. Tian, and F. J. a. p. a. Wu, "MFGNet: Dynamic modality-aware filter generation for RGB-T tracking," *arXiv preprint arXiv:10433*, 2021.
- [44] J. Mei, D. Zhou, J. Cao, R. Nie, and Y. Guo, "Hdinet: Hierarchical dual-sensor interaction network for rgbt tracking," *IEEE Sensors Journal* vol. 21, no. 15, pp. 16915-16926, 2021.
- [45] X. Xiao, X. Xiong, F. Meng, and Z. J. S. Chen, "Multi-scale feature interactive fusion network for rgbt tracking," *Sensors*, vol. 23, no. 7, pp. 3410, 2023.
- [46] Y. Wang, X. Wei, X. Tang, K. Yu, and L. Luo, "RGBT tracking using randomly projected CNN features," *Expert Systems with Applications*, vol. 223, p. 119865, 2023.

- [47] K. Yan, C. Wang, D. Zhou, and Z. Zhou, "RGBT Tracking via Multi-stage Matching Guidance and Context integration," *Neural Processing Letters*, pp. 1-15, 2023.
- [48] K. Yan, J. Mei, D. Zhou, and L. Zhou, "External-attention dual-modality fusion network for RGBT tracking," *The Journal of Supercomputing*, pp. 1-22, 2023.
- [49] F. Zhang, H. Peng, L. Yu, Y. Zhao, B. Chen, and Measurement, "Dual-Modality Space-Time Memory Network for RGBT Tracking," *IEEE Transactions on Instrumentation*, vol. 72, pp. 1-12, 2023.
- [50] C. Li, L. Liu, A. Lu, Q. Ji, and J. Tang, "Challenge-aware RGBT tracking," in *European Conference on Computer Vision*, 2020, pp. 222-237.
- [51] P. Zhang, J. Zhao, D. Wang, H. Lu, and X. Ruan, "Visible-thermal UAV tracking: A large-scale benchmark and new baseline," in *Proceedings of the IEEE/CVF Conference on Computer Vision and Pattern Recognition*, 2022, pp. 8886-8895.
- [52] P. Zhang, J. Zhao, C. Bo, D. Wang, H. Lu, and X. Yang, "Jointly Modeling Motion and Appearance Cues for Robust RGB-T Tracking," *IEEE Transactions on Image Processing*, vol. 30, pp. 3335-3347, 2021.
- [53] H. Kiani Galoogahi, A. Fagg, and S. Lucey, "Learning background-aware correlation filters for visual tracking," in *Proceedings of the IEEE international conference on computer vision*, 2017, pp. 1135-1143.
- [54] M. Danelljan, G. Bhat, F. Shahbaz Khan, and M. Felsberg, "Eco: Efficient convolution operators for tracking," in *Proceedings of the IEEE conference on computer vision and pattern recognition*, 2017, pp. 6638-6646.
- [55] I. Jung, J. Son, M. Baek, and B. Han, "Real-Time MDNet," *Computer Vision – ECCV 2018*, pp. 89-104.
- [56] Z. Zhang and H. Peng, "Deeper and wider siamese networks for real-time visual tracking," in *Proceedings of the IEEE/CVF conference on computer vision and pattern recognition*, 2019, pp. 4591-4600.
- [57] Y. Zhu, C. Li, B. Luo, J. Tang, and X. Wang, "Dense Feature Aggregation and Pruning for RGBT Tracking," in *Proceedings of the 27th ACM International Conference on Multimedia*, Nice, France, 2019, pp. 465-472.
- [58] Y. Gao, C. Li, Y. Zhu, J. Tang, T. He, and F. Wang, "Deep Adaptive Fusion Network for High Performance RGBT Tracking," in *2019 IEEE/CVF International Conference on Computer Vision Workshop (ICCVW)*, 2019, pp. 91-99.
- [59] Y. Zhu, C. Li, J. Tang, and B. Luo, "Quality-Aware Feature Aggregation Network for Robust RGBT Tracking," *IEEE Transactions on Intelligent Vehicles*, vol. 6, no. 1, pp. 121-130, 2021.
- [60] C. Li, C. Zhu, Y. Huang, J. Tang, and L. Wang, "Cross-modal ranking with soft consistency and noisy labels for robust RGB-T tracking," in *Proceedings of the European Conference on Computer Vision (ECCV)*, 2018, pp. 808-823.
- [61] J. Hyun, M. Kang, D. Wee, and D.-Y. Yeung, "Detection recovery in online multi-object tracking with sparse graph tracker," in *Proceedings of the IEEE/CVF Winter Conference on Applications of Computer Vision*, 2023, pp. 4850-4859.